The ISME Journal (2008) 2, 528–541

www.nature.com/ismej

ORIGINAL ARTICLE

Micro-scale observations of the structure of aerobic microbial granules used for the treatment of nutrient-rich industrial wastewater

Romain Lemaire[1], Richard I Webb[2] and Zhiguo Yuan[1]
[1]*Advanced Water Management Centre (AWMC), The University of Queensland, St Lucia, Queensland, Australia and* [2]*Centre for Microscopy and Microanalysis (CMM), The University of Queensland, St Lucia, Queensland, Australia*

The structure and function of aerobic microbial granules from a lab-scale sequencing batch reactor treating nutrient-rich abattoir wastewater were investigated. These wastewater-fed granules were examined using a wide range of micro-scale techniques including light microscopy, scanning and transmission electron microscopy, fluorescent *in situ* hybridisation (FISH) combined with confocal laser scanning microscopy and oxygen and pH microsensors, in conjunction with a range of measurements in the bulk liquid phase. Interesting structural features were observed in these granules that have not been reported in synthetic-fed granules. The complex nature of abattoir wastewater was suggested to be responsible for accelerating the breaking process of large mature granules due to a rapid clogging of the granules pores and channels and for the very diverse microbial community observed displaying specific spatial distribution throughout the granules. More importantly, the dissolution at lower pH of mineral complexes associated to the granule matrix of extracellular polymeric substances might have caused the structural damages observed on the granules even though some pH buffer capacity was observed inside these granules. Ciliate protozoa were found to be very abundant on the surface of these wastewater-fed granules, which could potentially assist with reducing the high levels of suspended solids usually present in the aerobic granular sludge effluent. All these observations provide support to future studies on aerobic granular sludge treating real wastewater especially with regard to the granule structure and the mechanisms involved in their formation.
The ISME Journal (2008) **2,** 528–541; doi:10.1038/ismej.2008.12; published online 7 February 2008
Subject Category: microbial engineering
Keywords: aerobic granule; electron microscopy; EPS structure; FISH; industrial wastewater; micro-scale

Introduction

Biological treatment is considered the most environment friendly and cost-effective way for removing organic compounds (often measured as chemical oxygen demand (COD)) and nutrients, such as nitrogen (N) and phosphorus (P), from wastewater streams. In conventional activated floccular sludge systems, microorganisms and small particles in the wastewater shape into small aggregates or flocs (50–300 μm in size). Under special condition, these aggregates can become much bigger and compact forming granules (0.3–5 mm). While granules were first reported in an upflow anaerobic sludge blanket bioreactor two decades ago (Lettinga *et al.*, 1980), recent research efforts have been dedicated to the study of aerobic granules (Morgenroth *et al.*, 1997; Beun *et al.*, 1999; Peng *et al.*, 1999; Etterer and Wilderer, 2001; Tay *et al.*, 2001). Aerobic granules cultivated in synthetic wastewater bioreactors have been reported to achieve COD and/or N removal (Tay *et al.*, 2002; Liu *et al.*, 2003; Yang *et al.*, 2003) and, in some cases, P removal (Dulekgurgen *et al.*, 2003; Lin *et al.*, 2003). Aerobic granules can be described as compact and dense aggregates of microbial origin with an approximately spherical external appearance that do not coagulate under reduced hydrodynamic shear and settle significantly faster than conventional activated sludge flocs. The main advantages of the aerobic granule technology are high biomass retention in the bioreactor, good settling properties and the capacity

Correspondence: Z Yuan, The University of Queensland, Advanced Water Management Centre, Gehrmann building, St Lucia, Queensland 4072, Australia.
E-mail: zhiguo@awmc.uq.edu.au
Received 11 October 2007; revised 4 January 2008; accepted 8 January 2008; published online 7 February 2008

to withstand high organic loading rates, which all contribute to the very small footprint of this technology in comparison to conventional floccular activated sludge systems.

Aerobic granules do not form naturally and must be cultivated in bioreactors under specific operating conditions providing strong selective pressures (Liu and Tay, 2004). The effects of several key operating parameters (for example, dissolved oxygen concentration, shear force, settling time, feast/famine regime and organic loading rate) on granule size and reactor performance were comprehensively investigated with several different carbon substrates (acetate, glucose and phenol) (Liu and Tay, 2004). The large microbial diversity found in aerobic granules has also led researchers to hypothesize that granulation is not a function of specific microbiological groups (Beun *et al.*, 1999). However, the exact mechanisms involved in the successive stages of the aerobic granulation process have not yet been fully explained.

So far, most of the research has been primarily focussing on macro-scale characterization of aerobic granular sludge systems, whether there were designed for COD removal only or for both COD and nutrient removal. Only few recent studies explored the micro-scale structure of aerobic granules (Liu *et al.*, 2004; Ivanov *et al.*, 2005; Wang *et al.*, 2005; Chen *et al.*, 2007a; Liu and Tay, 2007; Zheng and Yu, 2007). The majority of these studies focussed on extracellular polymeric substances (EPS) and its distribution within aerobic granules since non-biodegradable EPS appear to provide an architectural structure and mechanical stability for such granules (Wang *et al.*, 2007). Unfortunately, to date, all these micro-scale studies were performed on granular systems fed with synthetic wastewater containing a single carbon source (that is, mainly acetate) and operated for COD removal only. The ultimate goal of aerobic granular sludge technology is to treat real wastewater, either from domestic or industrial origin, which often contains diverse carbon sources along with a multitude of organic and inorganic compounds and some particulate matters. This complex nature of real wastewater and the different substrate-degradation rates are likely to have an effect on the structure of aerobic granules and their ability to remove COD and/or nutrients due to a change in the granule microbial communities affecting both the type of EPS produced and the mass transfer of substrate within the granule (Schwarzenbeck *et al.*, 2005).

The aim of this study is to make micro-scale observations of the structure and function of aerobic granules fed with real wastewater, providing support to future studies on granule structure and the mechanisms involved in their formation. The granules from a lab-scale sequencing batch reactor (SBR) fed with nutrient-rich industrial wastewater (Yilmaz *et al.*, in press) were employed in the study. The structure and function of granules were examined using a wide range of micro-scale techniques including light microscopy, scanning and transmission electron microscopy (SEM and TEM, respectively), fluorescent *in-situ* hybridization (FISH) combined with confocal laser scanning microscopy and oxygen and pH microsensors, in conjunction with a range of measurements in the bulk liquid phase. The work is, to our knowledge, the most comprehensive micro-scale study on wastewater-fed aerobic granules using a variety of multi-disciplinary tools. Some of the structural features observed provided support to the hypotheses made previously by other researchers from aerobic granules obtained with synthetic feed. Others initiated new hypotheses regarding the general and microbial structure and the fate of mature granules, the effect of pH on the granule structure stability and the possible role played by protozoa in the overall system performance. The work also provided some new directions and recommendations for further experimental studies on aerobic granules in relation to their structure and behaviour in real systems.

Materials and methods

Nutrient-rich industrial wastewater

The wastewater used in this study was from a local abattoir in Queensland, Australia. At this site, the raw effluent passes through four parallel anaerobic ponds before being treated in a SBR for biological COD and N removal. Anaerobic pond effluent from the abattoir was collected on a weekly basis and stored at 4 °C. The average concentrations of COD, ammonia and phosphate are presented in Table 1 together with the organic, N and P loading rates applied to the SBR.

Reactor operation and sampling of granules

The aerobic granule SBR had a working volume of 5 l and was operated in a temperature-controlled room (18–22 °C). It was operated on an 8 h cycle consisting of 18 min non-mixed feeding (3 l each cycle), 60 min mixed anaerobic/anoxic, 315 min mixed aerobic, 80 min mixed anoxic, 2 min settling and 5 min decanting periods. The dissolved oxygen level was controlled between 3.0–3.5 $mgO_2\,l^{-1}$ during the entire aerobic period using an on/off aeration control system. The hydraulic retention time was 13.3 h and the sludge retention time was kept around 15–20 days through the automatic wastage of 40 ml of mixed liquor in each cycle. The wastage was sometime suspended for couple of days to compensate for the volume of sludge sampled for some experiments. The pH in the system, which was recorded but not controlled, typically fluctuated between 7.0 and 8.6 over the cycle.

All the granules analysed in this paper were sampled during steady state operation, after the SBR had been operated for more than a year achieving

Table 1 Summary of reactor performance during steady state operation

Parameter	*Influent*		*Effluent*	
	Concentration ($mg\,l^{-1}$)	*Loading rate* ($g\,l^{-1}\,d^{-1}$)	*Concentration* ($mg\,l^{-1}$)	*Nutrient removal efficiency*
Total N	237.3	0.43	33.8	85.7%
NH_4-N	221.7	0.40	0.8	99.7%
Total P	34.3	0.062	9.0	73.8%
PO_4-P	33.6	0.060	0.6	98.3%
Total COD	1480	2.7	467	68.4%
Soluble COD	1072	1.9	162	84.8%
Soluble BOD_5	Not analysed		<2	—
TSS	205	—	306	—

Abbreviations: BOD, biological oxygen demand; COD, chemical oxygen demand.

stable COD, N and P removal. Granules were either sampled at the end of the anaerobic period or at the end of the SBR cycle. The SBR was initially seeded with aerobic granules obtained from another lab-scale SBR fed with synthetic wastewater (Lemaire *et al.*, 2008). During the first 40 days (that is, start-up period), the SBR was fed only with synthetic wastewater. The SBR was then fed with a mixture of abattoir and synthetic wastewater for the following 3 months (that is, transition period). The percentage of abattoir wastewater in the influent was gradually increased from 0% to 100% to allow the granular biomass to acclimatize to the high levels of nutrients present in the anaerobically pretreated abattoir wastewater. Finally, the SBR was fed only with anaerobically pretreated abattoir wastewater and steady state was reached rapidly (Yilmaz *et al.*, in press).

Owing to the presence of mineral complexes inside these wastewater-fed granules over the course of the SBR cycle (Yilmaz *et al.*, in press) and the dissolution of these complexes at lower pH, the effect of pH fluctuation on the granule structure stability was investigated in several anaerobic batch tests. For each batch test, 200 ml of a mixture of granule and liquor was sampled from the SBR at the end of the anaerobic period and transferred into a pH-controlled vessel kept under anaerobic condition. The vessel was consistently mixed and granules were sampled after 1 h for examination under light and electron microscopy to monitor their structure. Bulk liquid pH of 7.5 (pH in the SBR at the end of the anaerobic period) and 6.5 were tested.

Physico-chemical analysis

To monitor the granule structure and characteristics, granule size distribution and density were measured. To determine the volumetric size distribution of the granules, 30 ml of well-mixed granular sludge was sampled from the SBR at the end of the aeration period and pumped through a Malvern laser light scattering instrument, Mastersizer 2000 series (Malvern Instruments, Worcestershire, UK). The granule density, defined as the quantity of dry mass per biomass volume, was measured by the blue dextran method described in Lemaire *et al.* (2008), which was adapted from Di Iaconi *et al.* (2004).

The gradient of oxygen in granules was measured with oxygen microsensors (tip diameter $<10\,\mu m$), which were constructed as described by Revsbech (1989). Granules were sampled from the SBR at the start of the aerobic period when ammonia and phosphates were present at high concentrations and at the end of the aerobic period, at which time ammonia and phosphates were usually depleted. They were then transferred to a measuring-cell with an horizontal flow, where replicate oxygen profiles were measured using a microsensor mounted on a motor-controlled micromanipulator and averaged as described in Meyer *et al.* (2003). A diagram and full description of this measuring-cell can be found in Meyer *et al.* (2003). The composition of medium and the dissolved oxygen concentration in the measuring-cell was identical to that in the SBR at the start or the end of the aerobic period. The pH gradient in granules was measured with pH microsensors using the same experimental setup as that for oxygen profile measurement. Granules were sampled from the SBR at the end of the anaerobic period. The medium used in the measuring-cell was sampled from the SBR (liquid phase) at the same time to keep the substrate concentrations identical.

FISH probing

Granule samples were fixed, and were FISH probed as described previously (Amann, 1995). Prior to FISH probing, fixed granule samples were embedded in optimum cutting temperature compound (TissueTek, Sakura Finetek, Torrance, CA, USA) for cryosectioning as described previously (Meyer *et al.*, 2003). Embedded granules were then frozen and sectioned into 10-μm-thick slices using a cryotome

operated at −20 °C (Kryo 1720, Leitz, Wetzler, Germany). The granule sections were collected on SuperFrost Plus microscope slides (Menzel-Glaser, Braunschweig, Germany). Finally, the slides were dehydrated by sequential immersion for 3 min in 50%, 80% and 98% ethanol and air-dried.

The 16S rRNA-targeted oligonucleotide probes applied on the granule sections were the combination of EUB338 i–iii (EUBmix) for the detection of all bacteria (Daims *et al.*, 1999), the combination of PAO462, PAO651 and PAO846 (PAOmix) for *Accumulibacter* spp. (Crocetti *et al.*, 2000), the probe combination (GAOmix) of GAOQ989 (Crocetti *et al.*, 2002) and GB_G2 (Kong *et al.*, 2002) for *Competibacter* spp., NTSPA662 for *Nitrospira* spp. (Daims *et al.*, 2001), NIT3 for *Nitrobacter* spp. (Wagner *et al.*, 1996) and NSO1225 for most of the ammonia oxidizing bacteria (AOB) from the betaproteobacteria (Mobarry *et al.*, 1996). In addition, probes Actino-658 and Actino-221 for the newly proposed actinobacterial PAOs (polyphosphate-accumulating organisms) (Kong *et al.*, 2005) and DF988 and DF1020 for the *Defluviicoccus* spp.-related glycogen-accumulating organisms GAOs (Meyer *et al.*, 2006) were also used. Fluorescently labelled oligonucleotides were purchased from Thermo (Ulm, Germany) with fluorescein isothiocyanate or one of the sulfoindocyanine dyes indocarbocyanine or indodicarbocyanine.

Microscopy images

Whole fresh granules were photographed using an Olympus SZH10 stereo microscope with a DP70 digital camera.

Fluorescent *in situ* hybridization images were collected with a confocal laser scanning microscope Zeiss 510 (Carl Zeiss, Jena, Germany) using an argon laser (488 nm), a helium neon laser (543 nm) and a red diode laser (633 nm) fitted with 515–565 nm BP, 590 nm LP and 660–710 nm BP emission filters, respectively. To obtain images of entire granule sections, between 10 and 50 overlapping, consecutive images of 1024 × 1024 pixels were collected (depending on the size of the granule) using a Zeiss Neofluar × 40/1.3 oil objective. The final composite image of the granule section was then reconstructed from all the single images collected using Adobe Photoshop 7.0 (Adobe Systems, San Jose, CA, USA). For single images of specific part of the granule section a Zeiss Apochromat × 63/1.4 oil objective was used. FISH quantification was performed according to Crocetti *et al.* (2002), where the relative abundance of targeted group was determined using the pixel Measure/Count tool in Image Pro 4.0 (Media Cybernetics, Bethesda, MD, USA). Briefly, the area of pixels contributed by the FISH probes of the targeted group above a manually determined threshold was divided by the area of pixels contributed by the EUBmix probes (also applying threshold) for each granule section image. Individual pixels of the targeted group counted as 'positive' were also required to have a 'positive' pixel signal from EUBmix, above given thresholds.

To visualize the structure of aerobic granules at a micro-scale level, SEM and TEM were employed. Prior to visualization, granules EPS material was first stabilized using 2.5% glutaraldehyde and 75 mM lysine in 0.1 M cacodylate buffer for 10 min to minimize any structural damages arising from the dehydration procedure (Jacques and Graham, 1989). All subsequent processing was performed in a Pelco Biowave microwave oven. Granules were fixed in 3% glutaraldehyde in 0.1 M cacodylate buffer and after washing in 0.1 M cacodylate buffer, were postfixed in 1% osmium tetroxide.

For TEM studies, granules were dehydrated in a graded acetone series and embedded in Epon resin. Semi-thin sections of 500 nm were stained with 1% toluidine blue and 1% borax and viewed with an Olympus BX61 stereo microscope. Ultra-thin sections of 60 nm thickness were cut using a Leica Ultracut UC6 ultramicrotome and mounted on the Formvar-coated copper grids, stained with 5% uranyl acetate in 5% methanol and Reynolds lead citrate, and viewed using a JEOL 1010 TEM operated at 80 kV. To further reduce any possible artefacts coming from the fixation steps, some fresh granules were also frozen in a Leica EMPACT 2 high-pressure freezer and cryosubstituted at −85 °C over 2 days in 2% osmium tetroxide and 0.5% uranyl acetate in acetone. Specimens were then warmed to room temperature over 13 h, washed in acetone and embedded in Epon resin. Ultra-thin sections were cut and viewed by TEM as described above.

For SEM studies, granules were dehydrated in a graded ethanol series and infiltrated with the drying agent hexamethyldisilazane and left overnight to dry before being sputter coated with platinum. Viewing of samples was conducted using a JEOL 6300F SEM operated at 5–10 kV. To observe the internal structure, some dehydrated granules were taken from 100% ethanol, frozen in liquid N and fractured. These fractured granules were then thawed in ethanol, dried as described above and coated with platinum. The internal structure of granules were visualized by SEM as described above.

Results and discussion

General macro-characteristics of mature granules

Over the course of this study, the granular sludge SBR was in steady state and consistently removed 85%, 99% and 98% of the soluble COD, ammonia and phosphates present in the abattoir wastewater, respectively. The average COD and nutrient concentrations in the effluent are presented in Table 1. Biological oxygen demand test of filtered effluent ($< 2\ mg\ l^{-1}$) indicated that the effluent soluble COD is non-biodegradable. This implies that the abattoir

wastewater used in this study contained a non-biodegradable fraction of approximately 15% in its soluble COD. Due to their specific design (that is, short settling time and sludge wasting with the effluent), it is well-documented that granular sludge systems produce an effluent containing higher levels of suspended solids compared to floccular sludge systems. As a result, the total COD, total N and total P removal efficiencies were only 68%, 86% and 74%, respectively. This good nutrient removal was achieved through the process known as simultaneous nitrification, denitrification and P removal, likely facilitated by the presence of large and stable anoxic zones in the inner part of the granules where denitrification can occur. The oxidized N present at the end of the aerobic period was almost exclusively nitrite (data not shown) suggesting that most of the N was removed through nitrification and denitrification by nitrite in this granular SBR.

Figure 1 presents an overview of the macro-characteristics of the mature granules developed in this SBR fed with industrial wastewater. The volumetric size distribution of the granules presented in Figure 1a indicates that more than 80% of the biomass volume is made of granules with a size larger than 600 μm, whereas the volume percentage of biomass with a size smaller than 300 μm (likely flocs) is less than 5% demonstrating that granules were the dominant form of bacterial aggregates in this SBR. In comparison, the percentage volume of biomass with a size smaller than 300 μm in the same SBR before the granulation process was implemented was more than 90% (Figure 1a). The average density of these granules was measured at 150 g $l^{-1}_{biomass}$, which is considerably higher than what is generally reported for synthetic wastewater-fed granules (30–80 g $l^{-1}_{biomass}$). Figures1b and c show that most granules have a round shape with a clear outline; however, smaller granules with concave shapes were also observed suggesting they might have been part of a bigger granule that disintegrated, which will be further discussed later in this paper.

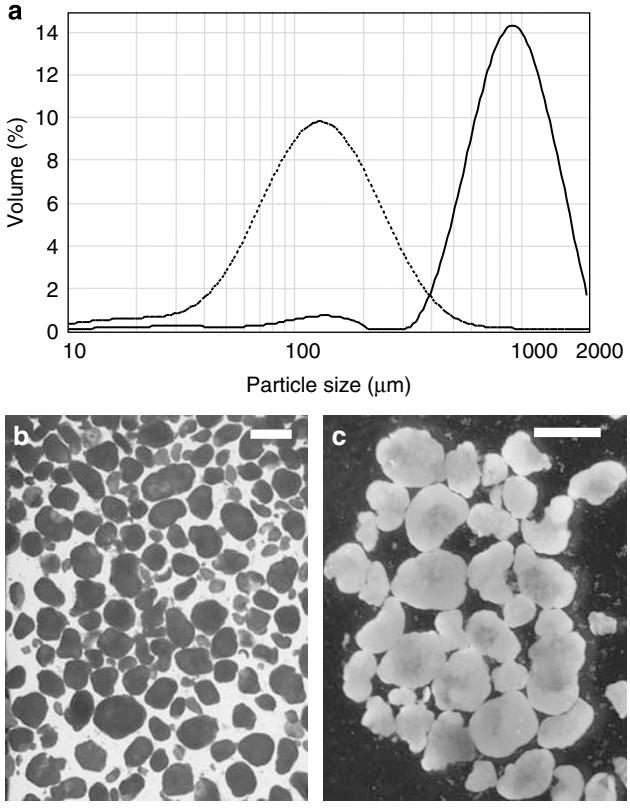

Figure 1 (**a**) Volumetric size distribution of the SBR before (dotted line) and after (solid line) granulation process was implemented and mature granules were formed. Pictures of granules obtained (**b**) with a scanner and (**c**) with a light microscope. Scale bars = 2 mm. SBR, sequencing batch reactor.

Micro-scale structure of granules and illustration of the role played by EPS

To explore the micro-scale structure of these granules especially in regards to the EPS structural matrix, electron microscopy (both SEM and TEM) was employed (Figure 2). The overall round shape of aerobic granules is actually made up of large cauliflower-like outgrowths (Figure 2a). These outgrowths have also been reported in acetate-fed aerobic granules (Tay *et al*., 2004; Liu and Tay, 2007), but were not as pronounced as observed in this study. On the surface of the granule (Figure 2c) some glue-like substances (that is, EPS), provide the cohesive material to maintain the bacteria bound to each other. To demonstrate the importance of the lysine-based prefixation step before visualizing granules with SEM, a SEM image of a granule that has not been prefixed in lysine solution is shown in Figure 2e. The EPS matrix has obviously shrunk during the dehydration process revealing more rod-shaped bacteria underneath it. Extreme caution should be exercised when preparing biological samples for SEM or TEM observation to avoid any structural artefacts. The internal EPS structure was observed on granules fractured in liquid N to prevent any structural damages coming from the use of a cutting tool. The SEM picture of the inner part of a fractured granule is presented in Figure 2b. Figure 2d presents a close-up image of the field delimited in black in Figure 2b, which is located near the surface of the granule. All bacterial cells visible on this image are embedded in the EPS matrix. The cellular origin of this EPS is clearly demonstrated in the high-magnification SEM image of a fractured granule displayed in Figure 2f. Each individual cell is enclosed in a thick EPS capsule. An ostensible difference can be made between the EPS of this cell capsule and the main EPS matrix cementing the overall granule. The real distance between bacteria in granules is very difficult to assess due to the thickness of the sections generally observed by light microscopy or confocal laser

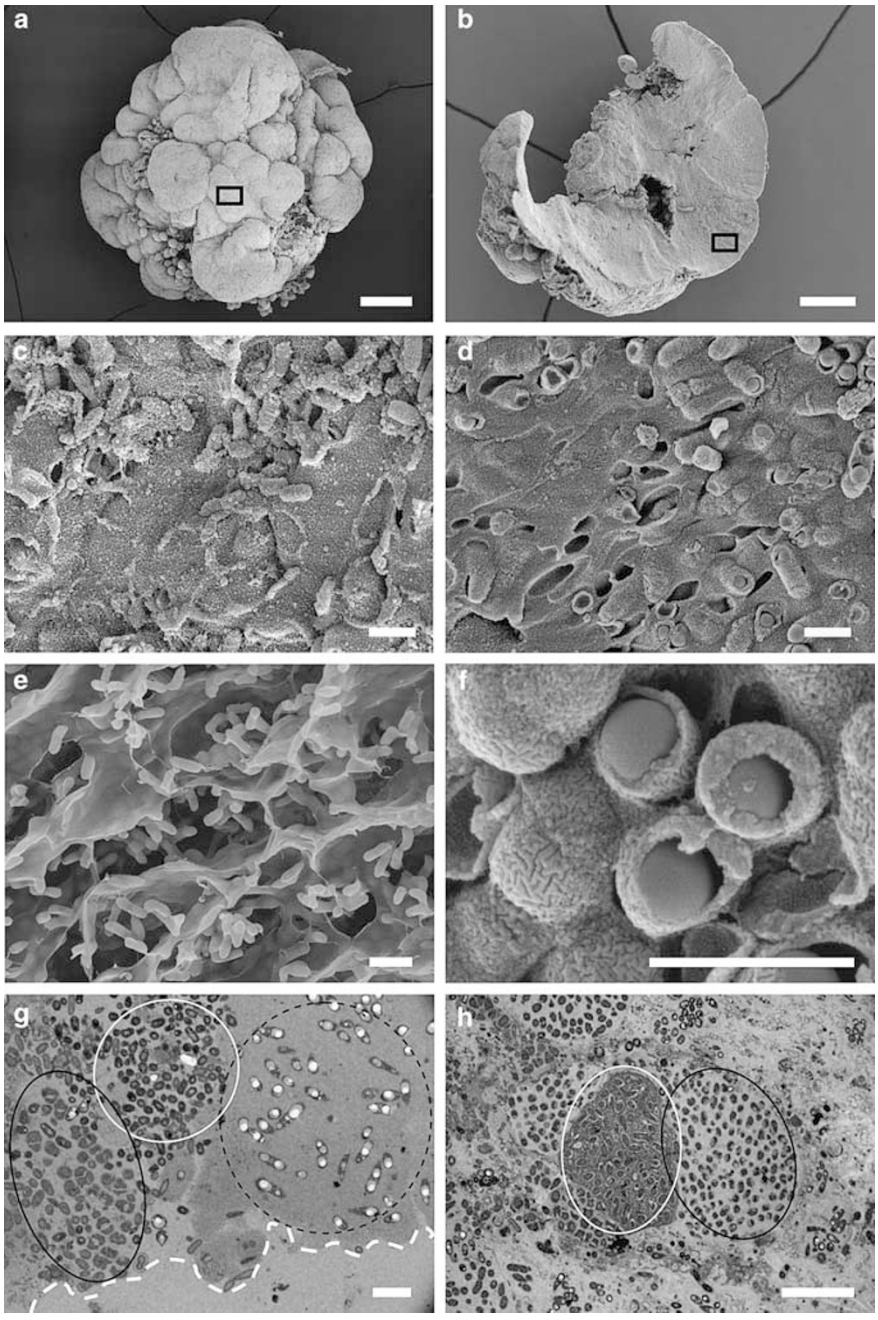

Figure 2 SEM images of (**a**) an entire granule, scale bar = 200 μm; (**b**) a fractured granule, scale bar = 200 μm; (**c**) granule outer surface delimited in black in (**a**), scale bar = 1 μm; (**d**) granule inner surface delimited in black in (**b**), scale bar = 1 μm; (**e**) outer surface of a granule without any prefixation step, scale bar = 1 μm; (**f**) granule inner surface at high magnification, scale bar = 1 μm; TEM image of (**g**) three bacteria clusters in the outer part of a granule, scale bar = 5 μm; (**h**) two bacteria clusters showing different types of EPS, scale bar = 5 μm. EPS, extracellular polymeric substances; SEM, scanning electron microscopy; TEM, transmission electron microscopy.

scanning microscopy, where lots of bacteria are piled up on the top of each other. The TEM image of a granule ultra-thin section depicted in Figure 2g reveals the exact distance between each cell in three different bacteria clusters defined by their size, shape, grey-scale intensity and general texture at high magnification. The cell-to-cell distance varied substantially depending on the type of bacteria resulting in sparse or dense cell clusters. The space between cells is filled by some EPS material, which means that the cells from the sparse cluster might indeed produce more EPS than those from the dense cluster. The type of EPS produce by different clusters of bacteria is also likely to be different throughout the granule. To illustrate this point, Figure 2h shows a TEM image of two different clusters of bacteria, one cocci-shaped and one rod-shaped, embedded in what appear to be different types of EPS matrixes based on the grey scale intensity and texture.

Voids, channels and fate of large mature granules

Voids and channels have been reported in some acetate-fed granules (Ivanov *et al*., 2005; Zheng and Yu, 2007) and were found to play a key role in the transport of substrate and metabolites in and out of the granules. Such voids or cavities were observed in almost every granule sections examined. One of these large voids can be seen in the centre of the granule section depicted in Figure 3a. These voids were most of the time connected to the outside of the granules through channels-like structures as illustrated in the light microscope images of Figure 3b and c and the TEM image of Figure 3d. The channels depicted in Figures 3c and d are filled with some material, again likely EPS, and could be compared to a ground water system where liquid can circulate in and out of the granules through some porous material. Very few clusters of bacteria are present in these channels probably due to the constant flow of liquid, which prevents them from attaching firmly on to the granule and thus being washed away. In comparison, the channel presented in Figure 3b is not filled with any material and appears to be more like an open river system where liquid can circulate more freely. These types of channels or interstices are usually located on the boundary line between two cauliflower-like outgrowths. The two large blue shapes at the entrance of this channel are two protozoa (ciliates from the Peritrich group) and their presence will be discussed later in this paper.

As mentioned earlier, not all granules in our SBR were big and round shaped. A large number of granules were of concave shape with smooth, dense cauliflower-like outgrowths on one side and loose and fluffy organization on the other. Some examples of such granules are presented in Figures 4a and b. A close-up image of the smooth and dense side of such a granule is shown in the Figure 4c, whereas the loose and fluffy side is shown in Figure 4d. These highly heterogenous granule structures seem to originate from the disintegration of bigger granules. The newly formed granules can then grow to become big mature granules that would break into smaller aggregates. However, the properties of these 'recycled' mature granules would likely differ from that of the original large mature granules due to the heterogeneity of the structure from which they had to re-develop. A recent research study by Zheng and Yu (2007) found a positive correlation between the bioactivity of acetate-fed granules and their porosity, and also reported that the granule porosity decreased as the granule size increased. They suggested that the pores of large granules were more readily plugged by EPS leading to a decrease of the biological activity because of a lack of nutrient or metabolite transport. In our system, the particulate and colloidal matter and the high level of fat, oil and grease present in abattoir wastewater might have speeded up the clogging process of the granule channels and pores and increased the mass transfer limitation of nutrients and substrates. This would have weakened the inner structure of the granule, and explain why our granules grew only to a maximum size of 1.5–2 mm before breaking up into

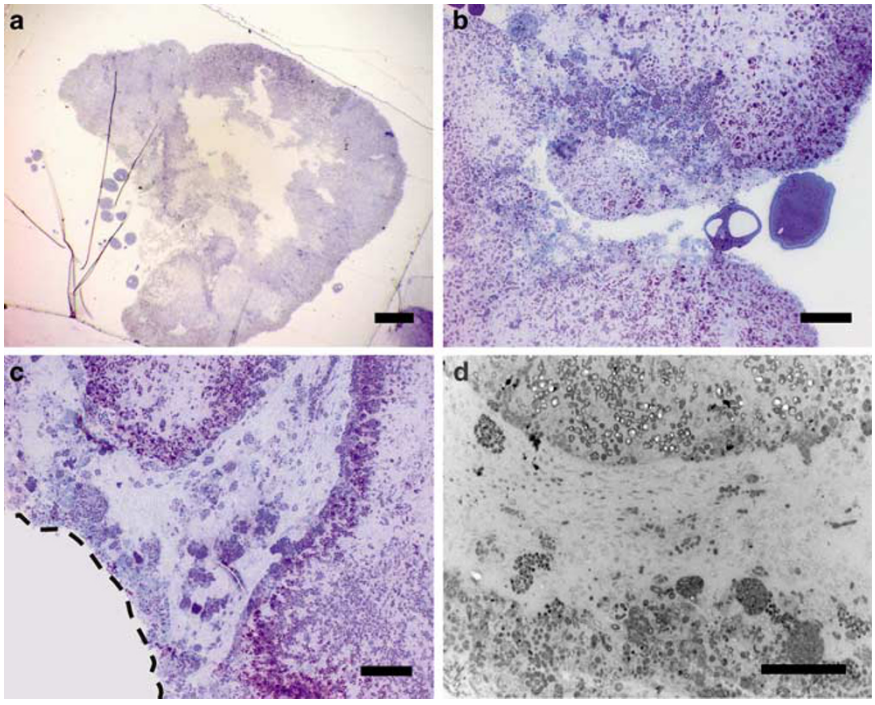

Figure 3 Light microscope images of semi-thin sections (500 μm) embedded in resin and stained with toluidine blue of (**a**) an entire granule, scale bar = 100 μm; (**b**) and (**c**) channels on the granule surface, scale bar = 10 μm; (**d**) TEM image of an inner channel, scale bar = 10 μm. TEM, transmission electron microscopy.

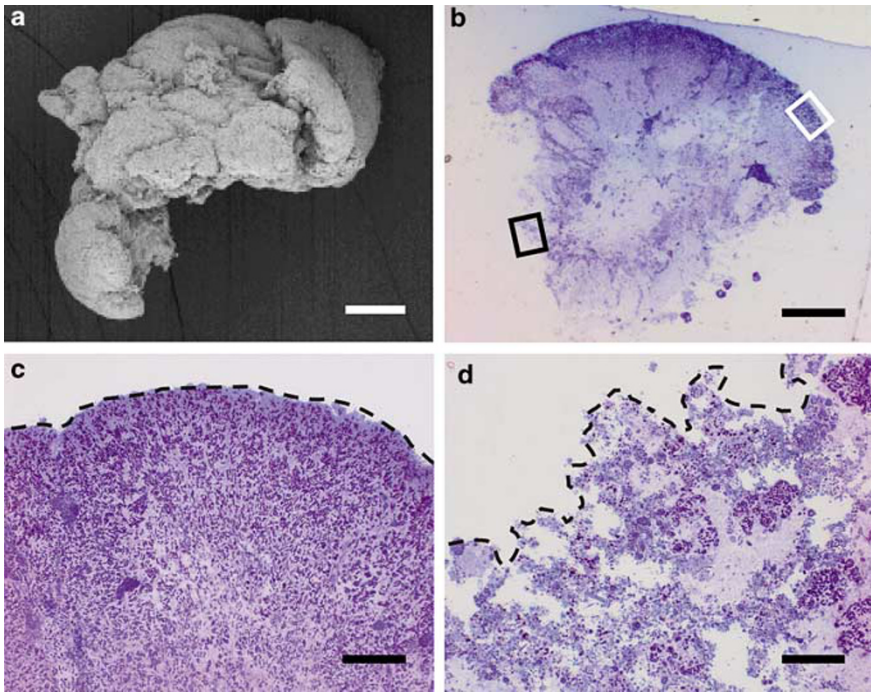

Figure 4 (**a**) SEM image of a broken granule, scale bar = 100 μm; light microscope images of semi-thin sections (500 μm) embedded in resin and stained with toluidine blue of (**b**) a broken granule, scale bar = 100 μm; (**c**) part of the granule edge delimited in white in (**b**), scale bar = 10 μm; (**d**) part of the granule edge delimited in black in (**b**), scale bar = 10 μm. SEM, scanning electron microscopy.

smaller and less homogenous granules. Therefore, not only the well-studied operating parameters such as settling time, shear force and organic loading rate can have an impact on the size of the granules, but also the characteristics of the wastewater to be treated.

Microbial population and distribution in granules

The mass transfer limitation of nutrient, substrates and metabolites inside the large granule was proposed to cause the breaking up of mature granules into smaller aggregates. This theory implies that the core part of mature granules must be deprived of any substantial microbial activity due to substrate diffusion limitation. Some researchers have used staining methods to establish the distribution profile of total (SYTO 63) and dead cells (SITOX Blue, *Bac*Light Live-Dead staining kit) in acetate-fed aerobic granules (McSwain *et al.*, 2005; Chiu *et al.*, 2007; Chen *et al.*, 2007b). The problem with these methods is that no standard procedure is available in the literature for the staining of entire granules and different incubation times, ranging from 5 to 30 min have been employed by different groups. Due to the diffusion limitation likely to occur in large granules, the time of incubation should probably be defined based on the size of the granules if anything. Due to the lack of consistency of these staining procedures, the cell distribution in our wastewater-fed granules was investigated qualitatively using SEM and TEM images. A SEM image of the central part of a fractured granule is illustrated in Figure 5a. This image can be compared to that of Figure 2f taken near the granule surface. The same kind of EPS capsule is observed in both images, but the shapes of the cells enclosed in these capsules are very different. Cells in the central part of the granules (Figure 5a) are malformed compared to the smooth round shaped cells of Figure 2f. It is very likely that these amorphous cells are indeed dead cells. To confirm that, several juxtaposing TEM images were taken from the edge to the centre of the granule. Figures 5b and c are two examples of what could be observed in the centre and on the edge of every granule, respectively. Mostly cell walls embedded in the EPS matrix are left in the central part of the granules, whereas lots of compact cells are located on the edge of the granule. This cell distribution in wastewater-fed granules supports the nutrient and substrate diffusion limitation theory, which may be the main cause for the breaking up of large mature granules.

The microbial diversity within the granule structure and spatial distribution of various groups of bacteria of importance to biological nutrient removal was investigated using a wide range of FISH probes designed to identify the most common microbial communities responsible for P and N removal in activated sludge performing nutrient removal. *Accumulibacter* spp., the main PAO found in biological P removal system, were dominant in these wastewater-fed granules (41% of all bacteria). This domination is illustrated in Figures 6a and b where FISH images of entire granule sections are

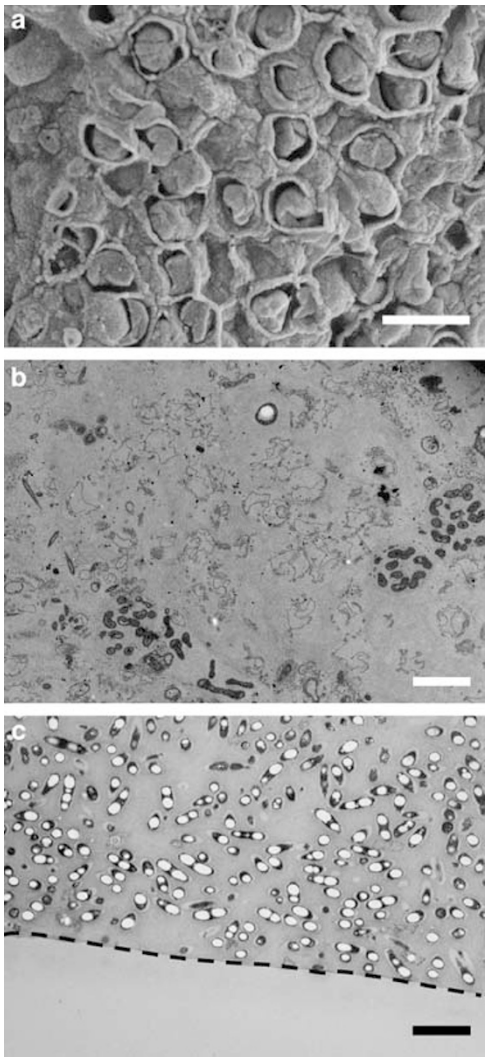

Figure 5 (**a**) SEM image of the central part of a fractured granule, scale bar = 1 μm; TEM images of (**b**) the central part of a granule section, scale bar = 5 μm; (**c**) the edge of the same granule section, scale bar = 5 μm. SEM, scanning electron microscopy; TEM, transmission electron microscopy.

reconstructed (*Accumulibacter* spp. in magenta, AOB in cyan and other bacteria in blue). Oxygen micro-profiles were measured in these granules during the first hour of the aeration period when the microbial activity was the highest (that is, substrates in excess) and at the end of the aeration period, 4 h later, when the microbial activity was lower (that is, most substrates depleted). Oxygen was found to penetrate only as far as 50 μm inside the granules in the first hour of the aeration period and around 400 μm deep at the end of the aeration (Yilmaz *et al.*, in press). *Accumulibacter* spp. were located on the outer part of these wastewater-fed granules where the dissolved oxygen concentration was higher. This preferred location has been already reported and quantified in acetate-fed granules performing N and P removal (Lemaire *et al.*, 2008). Other P removal microorganisms recently speculated, actinobacteria-PAO, were also present but in much lower abundance (4.1% of all bacteria) in comparison to *Accumulibacter* spp. as depicted in Figure 6c. Very few clusters of *Competibacter* spp. cells, the main GAOs usually found in large numbers in biological P removal processes, could be detected in the granules. This is considered desirable as GAOs compete with *Accumulibacter* spp. for the same carbon source but without performing any P removal. One of the few *Competibacter* spp. cluster present in these wastewater-fed granules is shown in Figure 6e in cyan.

The nitrifying organisms (that is, AOB and nitrite oxidizing bacteria (NOB), respectively) are also important microbial populations in nutrient removal processes due to their ability to oxidize ammonium/nitrite to nitrite/nitrate, which can then be reduced to dinitrogen gas by other organisms. AOBs were present in these granules as expected from the good nitrification performance of this SBR. A typical dense AOB cluster is depicted in Figure 6d in magenta. According to their strict aerobic metabolism, they should also be located on the outer part of the granule where oxygen is always available. Figures 6a and b show that most AOB clusters were indeed situated in the first 200 μm from the granule surface but rarely in the most outer part of the granule (that is, 0–50 μm layer), where oxygen availability is high. Instead, AOBs appear to grow just behind the thick layer of *Accumulibacter* spp. surrounding the granule edge. Strangely, some AOB clusters were even found right in the centre of the granule (indicated by the white circles on Figures 6a and b), where, according to the oxygen micro-profiles, oxygen should not be usually present. However, these AOB clusters were always located along the edge of large internal voids where small 'pockets' of oxygen might have been present after diffusing through some of the channels described earlier in this paper. This could explain why some oxygen micro-profiles presented small surges of oxygen concentration deep inside the granule. It clearly highlights the heterogenous nature of aerobic granules and the need to study a sufficient number of granules when investigating their micro-scale structure.

No NOB targeted by the FISH probes applied was found in these wastewater-fed granules. The oxidized N accumulating in the liquid phase of the SBR at the end of each cycle was almost exclusively nitrite (data not shown) confirming the absence of NOB in the system and that N was likely removed through the nitrite pathway. The limitation of oxygen transfer inside the granules could have advantaged the nitrite reducing organisms over NOB by providing large anoxic zones, where denitrification could occur using the soluble COD present in the wastewater. In addition, the domination of *Accumulibacter* spp. on the outer part of the granules, where oxygen was abundant, might have prevented NOB to adequately perform their aerobic metabolism due to insufficient oxygen availability.

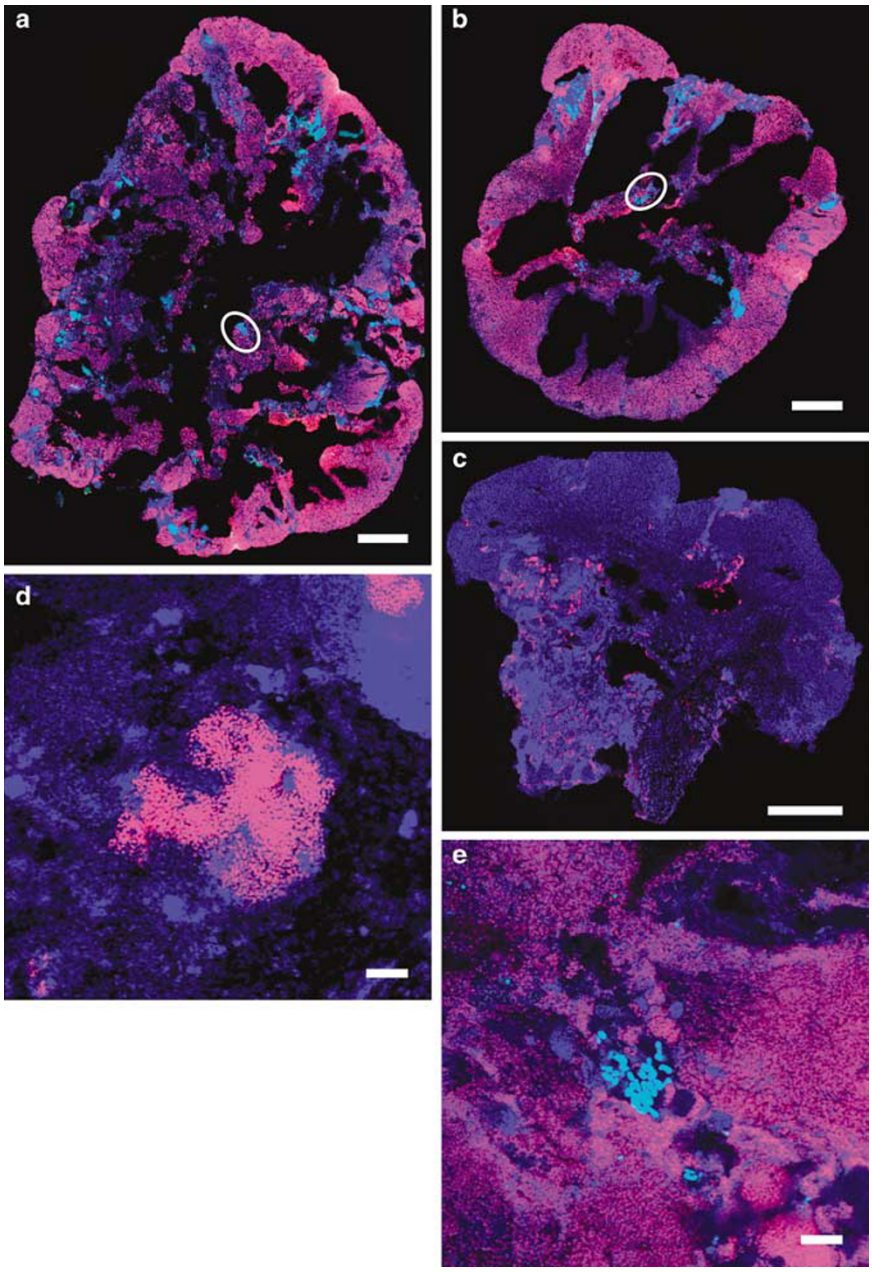

Figure 6 Reconstructed confocal laser scanning microscopy images of FISH micrographs of entire granule sections (**a–c**) and part of the section (**d** and **e**). In (**a**) and (**b**) *Accumulibacter* spp. cells are magenta (overlay of red PAOmix and blue EUBmix) most of the AOB from the betaproteobacteria are in cyan (overlay of green NSO1225 and blue EUBmix) and other bacteria are blue (blue EUBmix). The white circle highlights the presence of AOB in the centre of the granule. In (**c**) Actinobacteria PAO cells are magenta (overlay of red Actino-658 and blue EUBmix) and other bacteria are blue (blue EUBmix). In (**d**) AOB from the betaproteobacteria are in magenta (overlay of red NSO1225 and blue EUBmix) and other bacteria are blue (blue EUBmix). In (**e**) *Accumulibacter* spp. cells are magenta (overlay of red PAOmix and blue EUBmix) *Competibacter* spp. are in cyan (overlay of green GAOmix and blue EUBmix) and other bacteria are blue (blue EUBmix). Scale bars = 100 μm for (**a**), (**b**) and (**c**) and 10 μm for (**d**) and (**e**). AOB, ammonia oxidizing bacteria; FISH, fluorescent *in situ* hybridization; PAO, polyphosphate-accumulating organism.

Impact of bulk liquid pH on the granule structure

Aerobic granular sludge technology is particularly well-suited to treat industrial wastewater due to its small footprint and capacity to withhold high loading rates. Most intensive water user industries are subject to inherent production variability often resulting in changes of the wastewater composition, which could affect its pH. Yilmaz *et al*. (in press) reported that mineral complexes such as struvite and apatites could precipitate in these wastewater-fed granules during the anaerobic phase of the SBR cycle when the concentration of Ca^{2+}, Mg^{2+}, NH_4^+ and PO_4^{3-} ions is the highest. Owing to the dissolution of these complexes at lower pH and the possible effect that they could have on the overall granule structure, the influence of pH variation on the

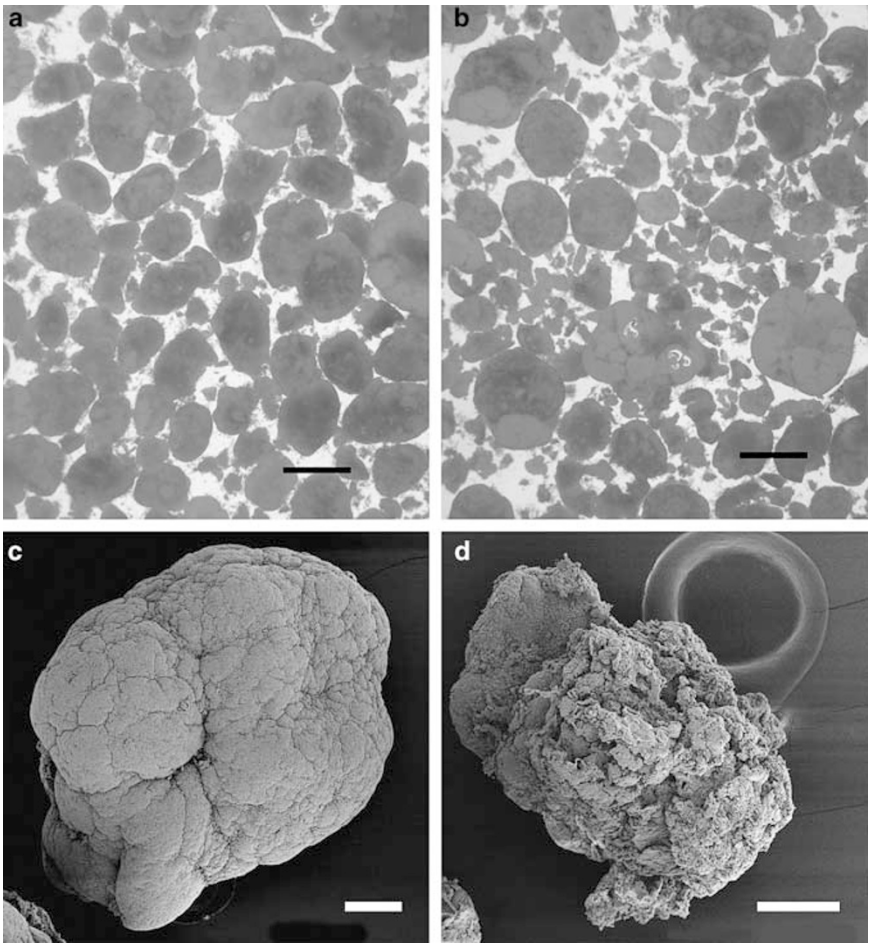

Figure 7 Light microscope images of granules after 1 h anaerobic batch test performed (**a**) at pH 7.5 and (**b**) at pH 6.5, scale bars = 1 mm. SEM images of the same granules after batch test (**c**) at pH 7.5 and (**d**) at pH 6.5, scale bars = 200 μm. SEM, scanning electron microscopy.

macro-structure of wastewater-fed granules was investigated. Series of batch tests were performed in a small pH-controlled vessel to investigate the effect of pH on the granule structure. Figures 7a and c show light microscopy and SEM images of the granules after a 1 h batch test at pH 7.5, simulating the bulk liquid pH of the SBR at the end of the anaerobic period, while example images obtained in the case of pH 6.5 are shown in Figures 7b and d. After 1 h batch test at pH 6.5, granules started to lose their smooth and compact external appearance (Figure 7d) and most of the smaller granules even completely disintegrated (Figure 7b). This disintegration led to a significant decrease of the volumetric size distribution of granules with the 10, 50 and 90th percentiles dropping by an average of 80%, 50% and 20%, respectively.

To better understand the effects that lower bulk liquid pH can have on the granule structure, microsensors were employed to measure the *in situ* pH profiles in these wastewater-fed granules after immersion in a pH-controlled flow cell. One of the several pH profile time series measured is presented in Figure 8. The first pH profile ($t = 0$) was measured as soon as the granule was transferred from the

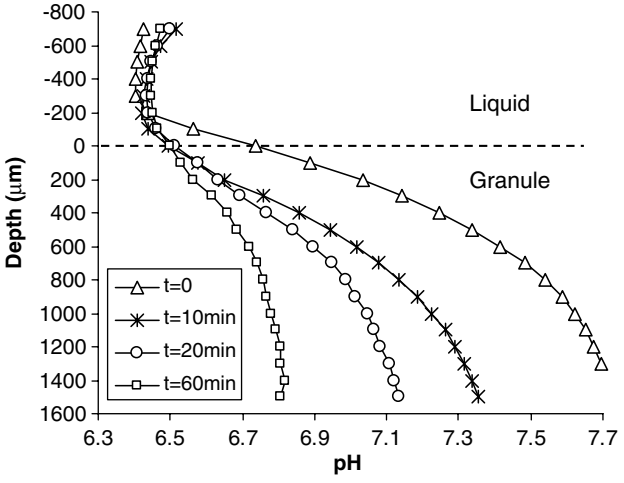

Figure 8 Typical pH profile time series measured in one granule using a microsensor in a flow-cell controlled at pH 6.5.

SBR bulk liquid (pH = 7.6) into the measuring-cell, where the pH was controlled at 6.5. The subsequent profiles were measured on the same granule (different location) after 10, 20 and 60 min. The presence of a clear pH gradient indicates that these granules

have a pH buffer capacity due to diffusion limitation and/or *in situ* biological activities. This buffering effect decreased overtime but a slight pH gradient remained visible even after 60 min. If the dissolution of mineral complexes likely associated with the granule's biopolymers (that is, EPS matrix) is indeed the main reason for the structural damage observed at lower pH, the presence of sharp pH gradient inside the granules would protect them from total disintegration. It could explain why during the batch tests at pH 6.5 small granules were more affected than large granules. The relatively limited pH buffer capacity of smaller granules would result in similar pH levels in the bulk liquid and in the granules and therefore increase their vulnerability under lower pH condition. Although these are only preliminary results, the high probability of having mineral complexes associated with the EPS matrix in granules treating nutrient-rich industrial wastewater calls for more extensive research to be done on the effect of dynamic pH fluctuations on the granule structural stability.

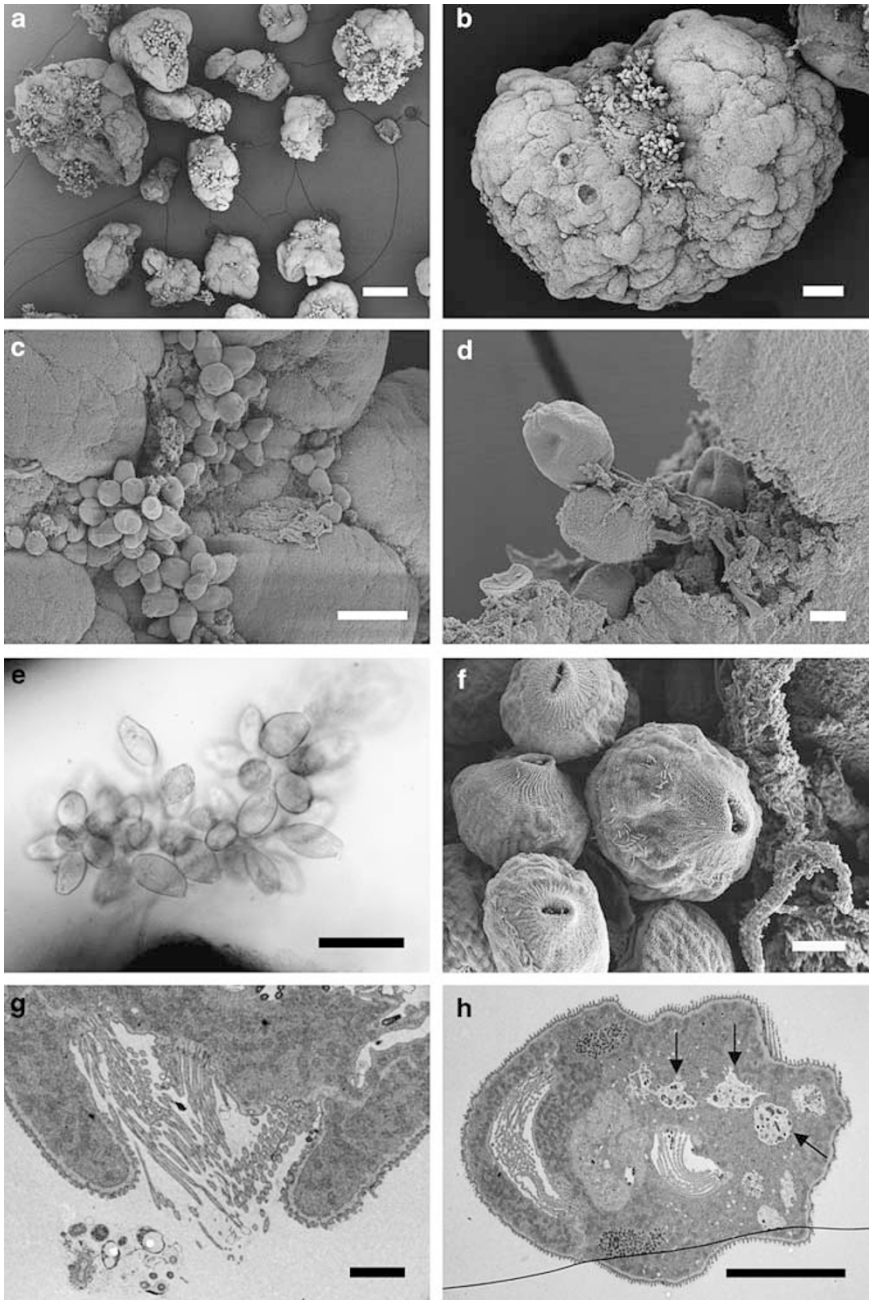

Figure 9 (**a–d**) and (**f**) SEM images of ciliates from the Peritrich group attached to the granule surface, scale bars = 1 mm (**a**), 200 μm (**b**), 100 μm (**c**) and 10 μm (**d**) and (**f**); (**e**) light microscope image of a bunch of ciliates, scale bar = 100 μm; TEM images of (**g**) oral cilia attracting free floating bacteria in the ciliate oral region, scale bar = 2 μm; (**h**) a ciliate cross-section with internal food vacuole indicated by the black arrows, scale bar = 10 μm. SEM, scanning electron microscopy; TEM, transmission electron microscopy.

Presence and role of ciliates on real wastewater-fed granules

Ciliates from the Peritrich group (likely from the *Opercularia* genus based on the observed morphology) were present in 'bouquets' on the surface of almost every granule examined (Figure 9a). These ciliates are attached to the granule through a stalk as depicted in Figure 9d. They are always located in the concave part of the granule (Figures 3a and 9b) or in interstices between large cauliflower-like outgrowths (Figure 9c). Due to the high shear force applied in the SBR, the constant collision between granules would have prevented ciliates to stay attached on the exposed part of the granules explaining why they are mostly located in sheltered areas.

The presence of these ciliates on the surface of the granules raises the question of their specific role and possible impact on the overall granular process. During measurement of oxygen profiles in granules, it was observed that when the microsensor tip had to progress through a ciliate bouquet before reaching the surface of the granule (Figure 9e), the measured oxygen concentration immediately dropped to zero. It indicates that ciliates were indeed interfering with the oxygen diffusion process in the granule by creating some localized oxygen-depleted zones at the surface of the granule. The high abundance of ciliates on each granule could have had an impact not only on the overall oxygen diffusion limitation in the granules but also on the diffusion of other substrates.

However, the main role of these ciliates in the system was probably related to their predatory behaviour. Like most protozoa, ciliates feed on small organic particulates including bacterial cells. They can sweep into their oral region (also called cytostome) free-floating bacteria by creating a vortex through the rotation of their oral cilia. The contracted peristome region of these ciliates can be observed in Figure 9f. The TEM image presented in Figure 9g shows a cross-section of the ciliate oral region with a group of free-floating bacteria close by. These bacteria are likely digested by the ciliate by the formation of internal food vacuoles that are depicted in Figure 9h (black arrows). High level of suspended solids in granular sludge effluent is a well-known drawback of the technology and post-treatments for solid's removal are often required (Schwarzenbeck *et al.*, 2005). It is directly linked to the process operation (that is, short settling time) where slowly settling biomass has to be washed out from the system continuously. The predation by these ciliates of the bacteria suspended in the SBR bulk liquid could help reduce the level of suspended solids discharged in the effluent at the end of each cycle and reduce the cost of post-treatments. More experimental work has to be done to estimate the fraction of suspended solids removed from the bulk liquid by these ciliates.

Concluding remarks

The structure of aerobic granules treating nutrient-rich wastewater in a SBR was investigated. Some interesting structural features were observed in these granules that have not been reported in synthetic-fed granules. The particulate and colloidal matter along with the fat, oil and grease present in abattoir wastewater appeared to have enhanced the breaking process of large mature granules due to a rapid clogging of the granules pores and channels. The various and complex types of substrates available also resulted in a more diverse microbial community compared to synthetic-fed granules with specific spatial distribution throughout the granules. This diverse community is likely to produce different sorts of EPS with different function. More importantly, the dissolution of mineral complexes associated to the granule EPS matrix at lower pH could indeed affect the structural stability of the granules. Further experimental studies are needed to understand the real impact of pH on the granule stability especially in regard to dynamic pH fluctuations as granules exhibit some *in situ* pH buffer capacity. Finally, the presence of ciliates on the surface of these wastewater-fed granules raises the question of their real contribution in removing small particulate matter from the bulk liquid. More targeted studies on that aspect could be beneficial for the overall aerobic granular sludge technology, which is known to produce an effluent with high levels of suspended solids.

Acknowledgements

This work was funded by the Environmental Biotechnology CRC, a Cooperative Research Centre established and funded by the Australian Government together with industry and university partners.

References

Amann RI. (1995). *In situ* identification of microorganisms by whole cell hybridization with rRNA-targeted nucleic acid probes. In: Akkermans ADL, van Elsas JD, de Bruijn FJ (eds). *Molecular Microbial Ecology Manual*. Kluwer Academic Publications: Dordrecht, Holland, pp 1–15.

Beun JJ, Hendriks A, van Loosdrecht MCM, Morgenroth E, Wilderer PA, Heijnen JJ. (1999). Aerobic granulation in a sequencing batch reactor. *Water Res* **33**: 2283–2290.

Chen MY, Lee DJ, Tay JH. (2007a). Distribution of extracellular polymeric substances in aerobic granules. *Appl Microbiol Biotechnol* **73**: 1463–1469.

Chen MY, Lee DJ, Tay JH, Show KY. (2007b). Staining of extracellular polymeric substances and cells in bioaggregates. *Appl Microbiol Biotechnol* **75**: 467–474.

Chiu ZC, Chen MY, Lee DJ, Wang CH, Lai JY. (2007). Oxygen diffusion in active layer of aerobic granule with step change in surrounding oxygen levels. *Water Res* **41**: 884–892.

Crocetti GR, Banfield JF, Keller J, Bond PL, Blackall LL. (2002). Glycogen accumulating organisms in laboratory-scale and full-scale activated sludge processes. *Microbiology* **148**: 3353–3364.

Crocetti GR, Hugenholtz P, Bond PL, Schuler A, Keller J, Jenkins D *et al.* (2000). Identification of polyphosphate-accumulating organisms and design of 16S rRNA-directed probes for their detection and quantitation. *Appl Environ Microbiol* **66**: 1175–1182.

Daims H, Bruhl A, Amann R, Schleifer KH, Wagner M. (1999). The domain-specific probe EUB338 is insufficient for the detection of all Bacteria: development and evaluation of a more comprehensive probe set. *Syst Appl Microbiol* **22**: 434–444.

Daims H, Nielsen JL, Nielsen PH, Schleifer KH, Wagner M. (2001). *In situ* characterization of Nitrospira-like nitrite oxidizing bacteria active in wastewater treatment plants. *Appl Environ Microbiol* **67**: 5273–5284.

Di Iaconi C, Ramadori R, Lopez A, Passino R. (2004). Preliminary biomass characterization in a sequencing batch biofilm reactor. *Ann Chim* **94**: 889–898.

Dulekgurgen E, Ovez S, Artan N, Orhon D. (2003). Enhanced biological phosphate removal by granular sludge in a sequencing batch reactor. *Biotechnol Lett* **25**: 687–693.

Etterer T, Wilderer PA. (2001). Generation and properties of aerobic granular sludge. *Water Sci Technol* **43**: 19–26.

Ivanov V, Tay STL, Liu QS, Wang XH, Wang ZW, Tay JH. (2005). Formation and structure of granulated microbial aggregates used in aerobic wastewater treatment. *Water Sci Technol* **52**: 13–19.

Jacques M, Graham L. (1989). Improved preservation of bacterial capsule for electron-microscopy. *J Electron Micros Tech* **11**: 167–169.

Kong Y, Ong SL, Ng WJ, Liu W-T. (2002). Diversity and distribution of a deeply branched novel proteobacterial group found in anaerobic-aerobic activated sludge processes. *Environ Microbiol* **4**: 753–757.

Kong YH, Nielsen JL, Nielsen PH. (2005). Identity and ecophysiology of uncultured actinobacterial polyphosphate-accumulating organisms in full-scale enhanced biological phosphorus removal plants. *Appl Environ Microbiol* **71**: 4076–4085.

Lemaire R, Yuan ZG, Blackall LL, Crocetti GR. (2008). Microbial distribution of *Accumulibacter* spp. and *Competibacter* spp. in aerobic granules from a lab-scale biological nutrient removal system. *Environ Microbiol* **10**: 354–363.

Lettinga G, Vanvelsen AFM, Hobma SW, Dezeeuw W, Klapwijk A. (1980). Use of the upflow sludge blanket (USB) reactor concept for biological wastewater-treatment, especially for anaerobic treatment. *Biotechnol Bioeng* **22**: 699–734.

Lin YM, Liu Y, Tay JH. (2003). Development and characteristics of phosphorus-accumulating microbial granules in sequencing batch reactors. *Appl Microbiol Biotechnol* **62**: 430–435.

Liu Y, Tay J-H. (2004). State of the art of biogranulation technology for wastewater treatment. *Biotechnol Adv* **22**: 533–563.

Liu Y, Yang SF, Tay JH. (2003). Elemental compositions and characteristics of aerobic granules cultivated at different substrate N/C ratios. *Appl Microbiol Biotechnol* **61**: 556–561.

Liu YQ, Tay JH. (2007). Characteristics and stability of aerobic granules cultivated with different starvation time. *Appl Microbiol Biotechnol* **75**: 205–210.

Liu YQ, Liu Y, Tay JH. (2004). The effects of extracellular polymeric substances on the formation and stability of biogranules. *Appl Microbiol Biotechnol* **65**: 143–148.

McSwain BS, Irvine RL, Hausner M, Wilderer PA. (2005). Composition and distribution of extracellular polymeric substances in aerobic flocs and granular sludge. *Appl Environ Microbiol* **71**: 1051–1057.

Meyer RL, Saunders AM, Blackall LL. (2006). Putative glycogen-accumulating organisms belonging to the Alphaproteobacteria identified through rRNA-based stable isotope probing. *Microbiology* **152**: 419–429.

Meyer RL, Saunders AM, Zeng RJX, Keller J, Blackall LL. (2003). Microscale structure and function of anaerobic-aerobic granules containing glycogen accumulating organisms. *FEMS Microbiol Ecol* **45**: 253–261.

Mobarry BK, Wagner M, Urbain V, Rittmann BE, Stahl DA. (1996). Phylogenetic probes for analyzing abundance and spatial organization of nitrifying bacteria. *Appl Environ Microbiol* **62**: 2156–2162.

Morgenroth E, Sherden T, van Loosdrecht MCM, Heijnen JJ, Wilderer PA. (1997). Aerobic granular sludge in a sequencing batch reactor. *Water Res* **31**: 3191–3194.

Peng DC, Bernet N, Delgenes JP, Moletta R. (1999). Aerobic granular sludge—a case report. *Water Res* **33**: 890–893.

Revsbech NP. (1989). An oxygen microsensor with a guard cathode. *Limnol Oceanogr* **34**: 474–478.

Schwarzenbeck N, Borges JM, Wilderer PA. (2005). Treatment of dairy effluents in an aerobic granular sludge sequencing batch reactor. *Appl Microbiol Biotechnol* **66**: 711–718.

Tay JH, Liu QS, Liu Y. (2001). Microscopic observation of aerobic granulation in sequential aerobic sludge blanket reactor. *J Appl Microbiol* **91**: 168–175.

Tay JH, Liu QS, Liu Y. (2002). Characteristics of aerobic granules grown on glucose and acetate in sequential aerobic sludge blanket reactors. *Environ Technol* **23**: 931–936.

Tay JH, Liu QS, Liu Y. (2004). The effect of upflow air velocity on the structure of aerobic granules cultivated in a sequencing batch reactor. *Water Sci Technol* **49**: 35–40.

Wagner M, Rath G, Koops H-P, Flood J, Amann R. (1996). *In situ* analysis of nitrifying bacteria in sewage treatment plants. *Water Sci Technol* **34**: 237–244.

Wang ZW, Liu Y, Tay JH. (2005). Distribution of EPS and cell surface hydrophobicity in aerobic granules. *Appl Microbiol Biotechnol* **69**: 469–473.

Wang ZW, Liu Y, Tay JH. (2007). Biodegradability of extracellular polymeric substances produced by aerobic granules. *Appl Microbiol Biotechnol* **74**: 462–466.

Yang SF, Tay JH, Liu Y. (2003). A novel granular sludge sequencing batch reactor for removal of organic and nitrogen from wastewater. *J Biotechnol* **106**: 77–86.

Yilmaz G, Lemaire R, Keller J, Yuan ZG. (in press). Simultaneous nitrification, denitrification and phosphorus removal from nutrient-rich industrial wastewater using granular sludge. *Biotechnol Bioeng* (doi: 10.1002/bit.21774).

Zheng YM, Yu HQ. (2007). Determination of the pore size distribution and porosity of aerobic granules using size-exclusion chromatography. *Water Res* **41**: 39–46.